Feature-Based Map Building Using Sparse Sonar Data in a Home-Like Environment

Se-Jin Lee
Department of Mechanical Engineering, Pohang University of Science and Technology, San 31 Hyoja-dong, Pohang 790-784, Korea
Jong-Hwan Lim
Department of Mechatronics, Cheju National University, #1 Ara-dong, Jeju 690-756, Korea
Dong-Woo Cho*
Department of Mechanical Engineering, Pohang University of Science and Technology, San 31 Hyoja-dong, Pohang 790-784, Korea

This study developed and implemented a new feature-based map-building model that uses only sparsely sampled sonar data from a fixed ring with 16 sonar sensors. It introduces two kinds of data filter approaches to overcome challenges associated with sonar sensors, such as a wide beam aperture and the specular reflection effect. The first approach is a footprint-association (FPA) model, which associates two sonar footprints into a hypothesized circle frame in order to determine the feature type, such as a line, a point, or an arc. The FPA model provides information about the trace of centers of hypothesized circles. It extracts features from a cluster composed of more than two independent footprints that originate from the same object. The other approach is a feature-association (FTA) model, which associates a new sonar footprint into extracted features to update the feature. Both proposed methods were tested in a home-like environment using a mobile robot.

Key Words : Data Filter Model, Feature Association, Feature-Based Map Building, Sparse Sonar Data

1. Introduction

Mobile robot navigation requires certain vital information, including a representation of the environment, localization, path planning, and obstacle avoidance. In most cases, building a map of an environment can be the basis for other functions used in autonomous navigation. Application of an environmental map allows a robot to recognize its position, obstacle locations and their geometric shapes, and the state of a working space (Thrun et al., 2004).

Typical sensors for building environmental maps include vision systems (Lee et al., 2005) and laser, infrared, and ultrasonic rangefinders. Researchers have used ultrasonic sensors extensively not only because these sensors are inexpensive but also because they provide direct depth information about object locations. Moreover, these sensors have a relatively long detection range and are unaffected by changes in light intensity. However, a sonar beam's specular reflection effect (Lim and Cho, 1994) results in the multipath phenomenon. This phenomenon, together with a wide beam aperture, makes it difficult to gather object locations using only a single sonar measurement.

* Corresponding Author,
E-mail : dwcho@postech.ac.kr
TEL : +82-54-279-2171; **FAX** : +82-54-279-5899
Department of Mechanical Engineering, Pohang University of Science and Technology, San 31 Hyoja-dong, Pohang 790-784, Korea. (Manuscript **Received** April 13, 2006; **Revised** October 17, 2006)

Researchers commonly use two different approaches to build sonar maps. The first approach is grid-based and divides the environment into several two-dimensional (2-D) or three-dimensional (3-D) cells. Each cell is represented by the probability of its being occupied by an object (Elfes and Moravec, 1985). Two typical techniques for building grid maps are the Bayesian updating model (Cho, 1990) and the orientation updating model (Lim, 1994; Lim and Cho, 1996). Use of a grid map is very efficient for representing object locations, regardless of object shapes, but building and maintaining a map of a large space requires considerable memory.

The other common approach is feature-based and represents the environment using three basic primitive geometries: a line, a point, or an arc. Crowley (1985) developed one of the earliest feature-based approaches by introducing the concept of the composite local model. This model used extracted straight-line segments from sets of sonar data and provided localization by matching them to a global line segment map stored previously. Wijk and Christensen (2000) later developed triangulation-based fusion (TBF) of sonar data, which delivers stable natural point landmarks. Nagatani et al.(1999) developed the arc transversal median (ATM) method and an arc carving algorithm. ATM and arc carving fused multiple sonar readings to improve azimuth resolution.

Leonard and Durrant-Whyte used a rotating sonar scanner to obtain densely scanned sonar data (Leonard, 1992), developing a simple threshold technique to extract regions of constant depth (RCDs) that were used to extract features such as lines and points. Kleeman (1999) designed a new sonar system based on a digital signal processor (DSP). This system was able to produce accurate measurements and on-the-fly single cycle classification of planes, corners, and edges.

This study developed and implemented a new feature-based map building model. The model does not use densely sampled sonar data from a rotating sensor; instead, it uses sparsely sampled sonar data from a fixed ring of 16 sonar sensors. Two kinds of data filter approach were developed to overcome two intrinsic challenges of using sonar sensors: the wide beam aperture and the specular reflection effect. One approach is a footprint-association (FPA) model, which associates two sonar footprints into a hypothesized circle frame in order to determine feature type such as line, point, or arc. The FPA model is able to provide information on the trace of centers of a hypothesized circle that is simultaneously tangential to the two circles defined by two sets of sonar range data. It clusters sets of data associated with identical primitive geometry and extracts a feature. The other data filter approach is the feature-association (FTA) model, which associates a new set of sonar data with extracted features in order to update feature information such as geometric shapes and their confidence rankings. During the study, both proposed methods were tested in a home-like environment using a mobile robot.

2. Ultrasonic Sensor

Sonar sensors can measure how far they are from the nearest object by using the elapsed time between a sonar beam's transmission and detection. Researchers have put a great deal of effort into building good quality sonar maps (Crowley, 1985; Elfes and Moravec, 1985; Cho, 1990; Lim, 1994; Lim and Cho, 1994, 1996). While some successes have been reported, results have largely been disappointing because ultrasonic sensors produce considerable angular uncertainty due to their wide beam aperture; they also suffer from the specular reflection effect (Lim, 1994; Lim and Cho, 1994, 1996).

Sonar beam power varies according to the angle from sensor bearings, as shown in Fig. 1. An

FIGURES

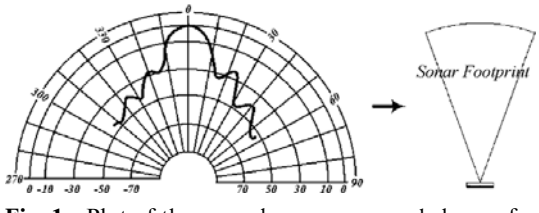

Fig. 1 Plot of the sonar beam power and shape of a sonar footprint. Note that dB is normalized to the on-axis response

angle at a power level of −6 dB is usually considered an effective beam aperture, so a sonar beam aperture is about 20–30°. A sonar beam has the approximate shape of a simple fan with an angle identical to the effective beam aperture ; we define this shape as the sonar footprint.

Ultrasonic sensors return a radial measure of distance to the nearest object within their range of detection. However, they frequently fail to detect the nearest object. There are two possible explanations for this (Lim and Cho, 1994 ; 1996). First, the object's surface may produce an echo amplitude that is too small to be detected by the receiver. Second, the echo pulse may be reflected away by a surface that is not perpendicular to the transducer axis. The latter, referred to as the specular reflection effect, happens more frequently. Since the surfaces of most real-world objects can be considered specular for ultrasonic sensors, this effect is almost always observed when the incidence angle is greater than half the beam's aperture (Lim, 1994).

Figure 2 presents measuring patterns of ultrasonic sensors according to the density of scanned data. The figure illustrates how the sonar sensors frequently do not detect walls due to the specular reflection effect. As shown in Fig. 2(e), it is possible to reduce both angular uncertainty and the specular reflection effect considerably by using densely scanned data to examine associations among neighboring sets of data. The RCD method is one simple and powerful means of reducing both the specular reflection effect and angular uncertainty (Leonard, 1992). However, these methods cannot be used when data are sparsely scanned because neighboring sets of these data have few associations. A single rotating sonar is usually applied to gather densely scanned data, but a single rotating sonar is not adequate for applications because it has a slow data acquisition speed. In addition, it requires a robot to stop when acquiring scanned data.

This study tested a sonar ring that gathered data quickly while a robot was in motion. In total, 16 sensors were mounted on the sonar ring, one every 22.5° (the effective beam aperture). As mentioned above, sparsely scanned data do not allow rejection of incorrect data corrupted by the specular reflection effect, and cannot reduce the sonar beam's angular uncertainty. To compensate for these challenges, we developed data filter models among the sonar footprints acquired at different scanning steps.

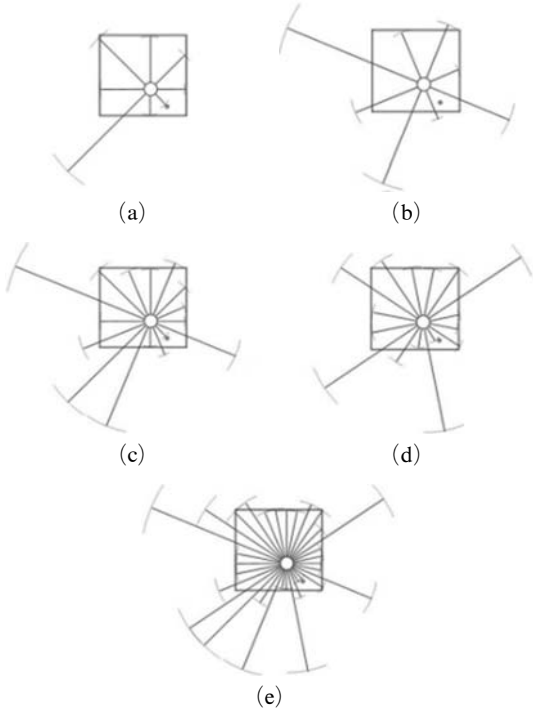

Fig. 2 Measurement pattern according to the number of sensors in a sonar ring and robot bearings : (a) 8 sonar sensors with 0° of robot bearings, (b) 8 sonar sensors with 22.5° of robot bearings, (c) 16 sonar sensors with 0° of robot bearings, (d) 16 sonar sensors with 11.3° of robot bearings, and (e) 32 sonar sensors with 0° of robot bearings. The sparse sonar data resulted in a remarkable change in vehicle orientation

3. Data Filter Models

We tested two kinds of data filter model to overcome the problems of wide beam aperture and the specular reflection effect. One was a footprint-association (FPA) model, which associates two sonar footprints into a hypothesized feature such as a line, a point, or an arc. This model

provides information about associated features. The other was a feature-association (FTA) model, which associates a new sonar footprint into extracted features to update geometric information.

3.1 Footprint-association (FPA) model

Sonar range readings generally contain considerable angular uncertainty because of their wide beam angle aperture. In addition, sonar sensors often produce false readings due to specular reflection of sound waves. Association of more than two sets of sonar data is therefore very important to prevent false readings and reduce angular uncertainties. Application of the FPA model allows determination of whether two sonar footprints are associated with a line, a point, or an arc. As shown in Fig. 3, sonar footprints that correspond to a plane or a cylinder should all be tangential to that plane or cylinder, while sonar footprints that correspond to a corner or an edge should all intersect at a corner or edge point (Leonard, 1992).

The FPA model basically estimates the possibility that two sets of sonar data originate from the same feature. For the example shown in Fig. 4, we can define two circles centered at sensor locations with radii equal to footprint range values, z_1 and z_2, and define the effective sonar beam aperture as each footprint's constraint angle, represented by the shaded fan shape. We can define a local coordinate system, centered at sensor location 1 (point O in Fig. 4), with sensor location 2 (point B in Fig. 4) on the positive x-axis at position $x=d$, where d is the distance between the two sensor locations. The FPA model assumes that if any two sets of range data, z_1 and z_2, originate from the same object, a hypothesized feature should define the third circle, which is tangential to the two circles defined by the footprints (Leonard, 1992). The general problem therefore is to find radius R of the third circle that defines the hypothesized feature. If the value of R approaches zero, the hypothesized feature should be a point, while if the value of R is infinite we can expect a line feature.

Let ϕ be the bearing from the original of the local coordinate system to the center of a hypothesized circle. We can get ϕ_1 using the law of cosines such as Eq. (1):

$$\phi_1=\cos^{-1}\left(\frac{(z_1+R)^2-(z_2+R)^2+d^2}{2d(z_1+R)}\right). \quad (1)$$

Unfortunately, we cannot uniquely determine the third circle because both R and ϕ are unknowns. Leonard developed very simple method to determine the third circle (Leonard, 1992). That is, he found ϕ_1 by taking the limit as $R\rightarrow$ infinite and $R\rightarrow 0$ respectively. As a result, the method can only be applied in the special case

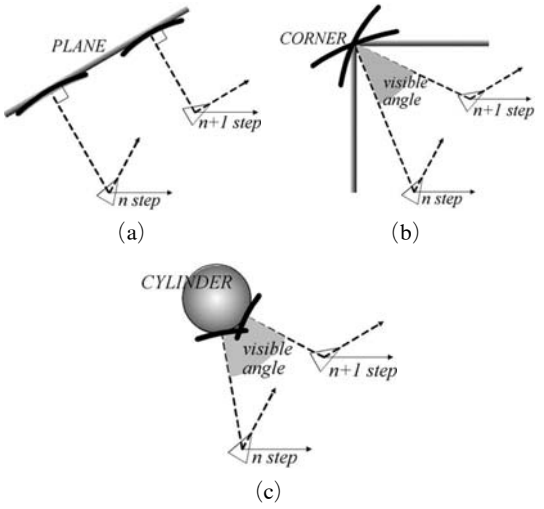

Fig. 3 Sonar footprints corresponding to (a) a plane, (b) a corner, and (c) a cylinder

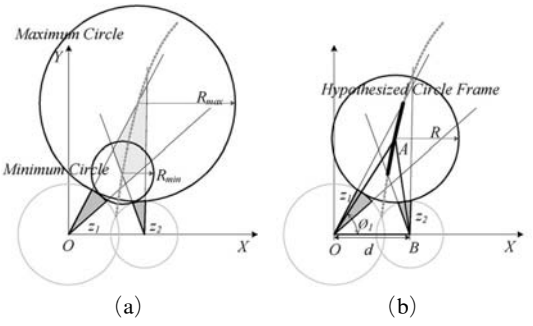

Fig. 4 Hypothesized circles that are tangential to the two circles defined by the footprints: (a) possible radius range for the hypothesized circles without considering angle constraints, and (b) trace of virtual circles' centers that satisfy the angle constraints

of line and point targets. We generalized the method by considering that bearing ϕ for each sensor footprint must simultaneously satisfy the angle constraint defined as an effective beam aperture. This fact makes it possible to calculate the bearing range, i.e., $\phi_{\min}$ and $\phi_{\max}$, and the corresponding $R_{\min}$ and $R_{\max}$. The bold solid line segment in Fig. 4, defined as the center line, represents possible center locations of the hypothesized circles with radii between $R_{\min}$ and $R_{\max}$.

It is possible to determine the bearing of a hypothesized circle uniquely for some special cases. If $R_{\min}$ is very large or approaching infinity, the two footprints are clustered into a line feature, and the corresponding bearing is calculated as Eq. (2):

$$\phi_1=\cos^{-1}\left(\frac{z_1-z_2}{d}\right). \tag{2}$$

In contrast, if $R_{\max}$ is very small or approaching zero, the footprints are clustered into a point, and ϕ_1 is calculated as Eq. (3):

$$\phi_1=\cos^{-1}\left(\frac{z_1^1-z_2^2+d^2}{2dz_1}\right). \tag{3}$$

Otherwise, the footprints are clustered into an arc feature. In this case, it is not possible to determine the hypothesized circle uniquely with only two sets of sonar data. If another set of sonar data is available that is associated with the same arc feature, the hypothesized circle can be determined uniquely by calculating the cross point of the two center lines. Section V discusses this process in more detail.

3.2 Feature-association (FTA) model

Using the FPA model explained above, all sonar readings that correspond to the same feature are clustered together. Tentative features are then extracted from the clusters and promoted to confirmed features according to the number of sonar data supporting the same hypothesized feature (Leonard, 1992). Once a tentative feature has been extracted, a footprint association is no longer required because that association was only used to determine the tentative feature; at this point, a feature of the footprint association (FTA) model is instead required.

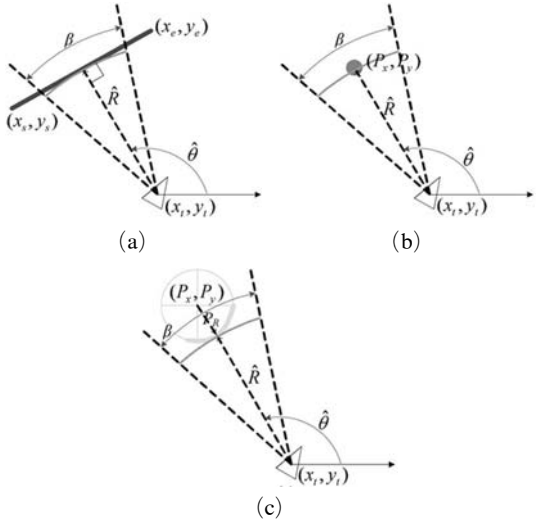

Fig. 5 Predicted footprints corresponding to (a) a line, (b) a point, and (c) an arc feature

The FTA model tests whether it is possible for a footprint to have originated from the given tentative feature. Figure 5 shows the predicted footprint, i.e., predicted range $\hat{R}$ and bearing $\hat{\theta}$ for each feature type. If the footprint satisfies the angle and range constraints given below, the FTA is successful.

$$|R-\hat{R}|\le\delta_R \text{ and } \theta_l\le\hat{\theta}\le\theta_u. \tag{4}$$

In Eq. (4), R is the measured range, and δ_R represents parameters to be designed based on sensor resolution. If the bearing of the sensor that produces range R is θ_m, then θ_l and θ_u are defined as Eq. (5):

$$\theta_l=\theta_m-\frac{\omega}{2},\ \theta_u=\theta_m+\frac{\omega}{2}. \tag{5}$$

ω is the effective beam width of sonar.

An occlusion test is performed for range data that satisfy FTA, and if the corresponding feature is not occluded it is updated. If the updated feature is tentative, it will be promoted to a confirmed feature if it satisfies the given conditions.

4. Extraction of a Line or Point Feature

The parameters that characterize a line feature are two end points and the visible direction;

the parameters of a point feature (a corner or an edge) include point position and visible direction. The visible direction of a line feature, defined as normal direction of the line, represents which side of the line is visible. In contrast, the visible direction of a point feature represents the angle range within which a robot can perceive the feature.

Figure 6 shows how line and point features are extracted and promoted. Sets of sonar data that support the same feature are clustered together using the FPA model. For feature promotion, we applied the procedure proposed by Leonard (1992), in which any cluster with more than four sets of sonar data is promoted to a tentative feature and if a cluster has six data sets, the tentative feature is promoted to a confirmed one.

The two end points of a confirmed line feature are calculated from the two sets of data corresponding to the end points, and the visible direction is found by calculating the normal direction from the sensor position to the line. In contrast, the position of a confirmed point feature is determined from the intersection of cluster footprints, and the visible direction of the feature is defined by the minimum and maximum sensor bearings among the cluster footprints.

When using the FTA model, a confirmed feature is updated whenever a new set of data supporting the feature appears. Only the two end points of a line feature and visible direction of a point feature are updated if necessary. The visible direction of a line feature and position of a point feature are not updated because they do not change and they could be corrupted by a robot's angle and position errors, which tend to accumulate as robots move.

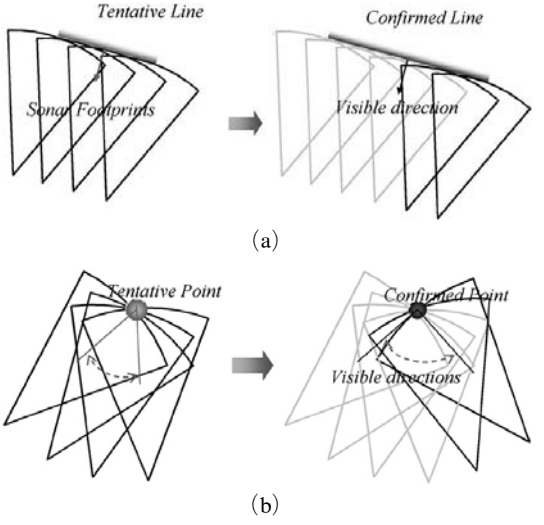

Fig. 6 Extraction of (a) a line and (b) a point features. The line is characterized by two end points and visible direction. The point line is characterized by the intersection point and range of visible angles (visible directions)

5. Arc Feature Extraction

The extraction of a line or point feature is a special case in which the radius of the hypothesized circle approaches infinity or zero, so uncertainty about the radius is minimized even though sonar footprints produce considerable angular uncertainties. In the extraction of an arc feature, however, the radius of a hypothesized circle is not limited except for its range of $R_{\min}$ and $R_{\max}$, as defined in section III. This study developed new approaches to extract and update arc features from sparsely sampled sonar data. Three parameters define an arc feature : the center location, the radius, and visible angles corresponding to the angle of a circular arc. After the initial parameter values are determined using three sets of sonar data at different positions, they are continually

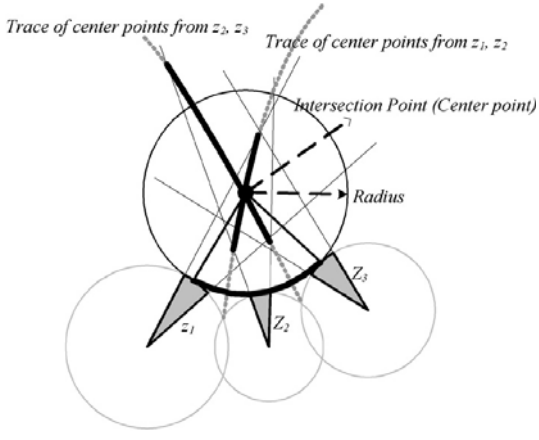

Fig. 7 Geometric relation for the arc feature extraction

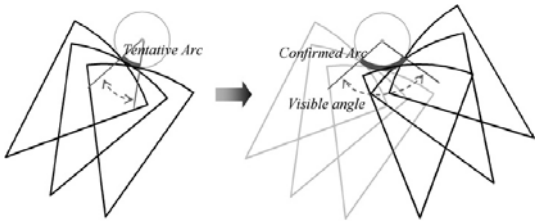

Fig. 8 Promotion of an arc feature

updated using the FTA model.

Figure 7 presents the geometric relationships for arc feature extraction. Using the FPA model, we can calculate the trace of center points using z_1 and z_2, and can determine the range of trace, the thick solid line in Fig. 8, using $R_{\min}$ and $R_{\max}$ as defined in section II. Likewise, we can determine the range of trace using z_2 and z_3. We can then find the intersection of the two traces. If the point of intersection exists within both ranges of traces, they are classified as a new tentative arc feature. If more than four sets of footprints consistently support the same arc feature, the arc feature is promoted to a confirmed one. The confirmed arc feature is continuously updated whenever a new footprint supporting the FTA model appears, as shown in Fig. 8.

6. Experimental Results

The proposed map building methods were implemented and tested in a real home environment with a mobile robot. The mobile robot used in these experiments was the Pioneer 3-DX, built by the ActiveMedia Robotics Company. A sonar ring composed of 16 sonar sensors at uniform intervals of 22.5° was mounted on top of the robot. The sonar sensor was a Polaroid 600 Series with a beam aperture of approximately 22.5°, a minimum detection range of 10 cm, and a maximum detection range of 10 m. Figure 9 shows the experimental environment, which consisted of sofas, tables, bookshelves, a clothes chest, chairs, an ashtray, and a fire extinguisher. Table and chair legs had diameters of 6 cm and 4 cm, respectively. A remote controller was used to program the robot to move along the area represented by a dashed line in Fig. 9, and no localization was

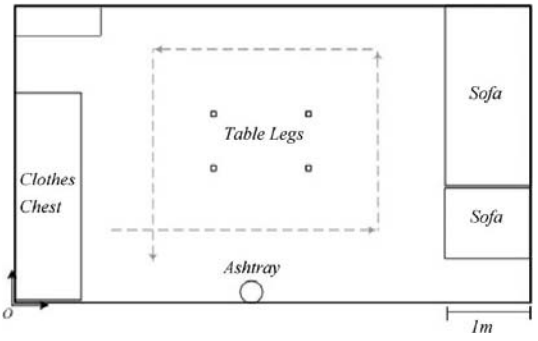

Fig. 9 Configuration of the experimental environment

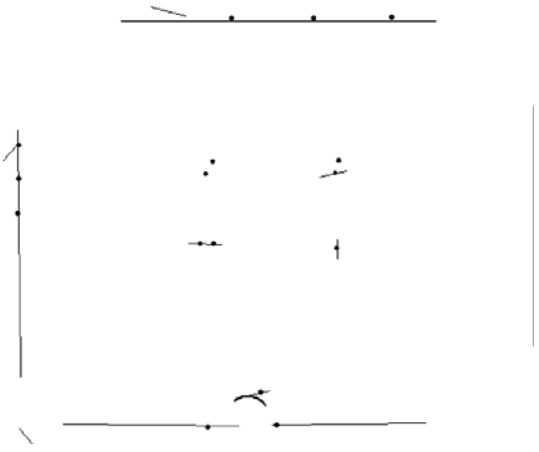

Fig. 10 Experimental results of feature mapping

applied. In total, 2800 data points were collected from 175 different positions; however, after applying the FPA model, only 474 sets of data were used to extract the features.

Figure 10 presents the mapping results after the robot made a complete circuit of the environment. Solid lines, dots, and the solid arc represent line features, point features, and an arc feature, respectively. Some unexpected line features appeared in the resulting map. This type of false line feature can appear when the distance between any two point features is very small. This problem is clearly illustrated by the small table and chair legs in the middle of the environment; these were estimated as both line and point features. These false lines are outliers to be rejected. The ashtray, which was shaped as a cylinder, was estimated as only a partial arc feature. This occurred because

the robot moved in a straight line as shown in Fig. 9, so it could not perceive the other side of the cylinder. One can see the line segments or points around the corners were hardly recovered. This is because of the well known 'corner problem of sonar sensors' due to specular reflection effect at the corner. In total, 25 line features, 37 point features, and 1 arc feature were identified. Considering the uncertainties of sonar sensors and the sparse sonar data, the quality of the resulting map was relatively good for navigation of the mobile robot.

7. Conclusions

This study developed and implemented a new feature-based map building model that does not use densely scanned sonar data from a rotating sensor but instead uses sparsely sampled sonar data from a fixed ring with 16 sonar sensors. It introduced two kinds of data filter approaches, FPA and FTA, to overcome the challenges of sonar sensors such as the wide beam aperture and the specular reflection effect. One approach was the FPA model, which associates two sonar footprints into a hypothesized circle frame to determine the feature type such as a line, a point, or an arc. In this model, tentative features are extracted from clusters composed of more than two independent footprints supporting the same hypothesized feature. The other approach was the FTA model, which associates a new sonar footprint into existing tentative or confirmed features to update their geometric information or promote them to confirmed features.

The developed methods were implemented and tested in a real home environment using a real robot. Results indicated that the resulting map quality is sufficiently for navigation of a mobile robot. Therefore, the proposed method of feature map building could be applied to simultaneous localization and mapping (SLAM) of a mobile robot.

Acknowledgments

This research was supported by the Home Service Robots Project of the Ministry of Information and Communication and the National Research Laboratory Program of the Ministry of Science and Technology, the Republic of Korea.

References

Cho, D. W., 1990, "Certainty Grid Representation for Robot Navigation by a Bayesian Method," *ROBOTICA*, Vol. 8, pp. 159～165.

Crowley, J. L., 1985, "Navigation for an Intelligent Mobile Robot," *IEEE J. of Robotics and Automation*, RA-1(1), pp. 31～41.

Elfes, A. and Moravec, H. P., 1985, "High Resolution Maps From Wide Angel Sonar," *IEEE Intl. Conf. on Robotics and Automation*, pp. 116～121.

Kleeman, L., 1999, "Fast and Accurate Sonar Trackers Using Double Pulse Coding," *IEEE/RSJ International Conference on Intelligent Robots and Systems*, pp. 1185～1190.

Lee, K. H. Kim, S. H. and Kwak, Y. K., 2005, "Mobility Improvement of an Internet-Based Robot System Using the Position Prediction Simulator," *Intl. J. of Precision Engineering and Manufacturing*, Vol. 6, No. 3, pp. 29～36.

Leonard, J. J., 1992, Direct Sonar Sensing for Mobile Robot Navigation, *Kluwer Academic Publishers*, Dordrecht, The Netherlands.

Lim, J. H. and Cho, D. W., 1994, "Specular Reflection Probability in the Certainty Grid Representation," *Trans. of the ASME*, Vol. 116, pp. 512～520.

Lim, J. H. and Cho, D. W., 1996, "Multipath Bayesian Map Construction Model From Sonar Data," *ROBOTICA*, Vol. 14, pp. 527～540.

Lim, J. H., 1994, "Map Construction, Exploration, and Position Estimation for an Autonomous Mobile Robot Using Sonar Sensors," *PhD dissertation*, Pohang Institute of Science and Technology, Korea.

Nagatani, K., Lazar, N. A. and Choset, H., 1999, "The Arc-Transversal Median Algorithm: An Approach to Increasing Ultrasonic Sensor Accuracy," *IEEE Intl. Conf. on Robotics and Automation*, pp. 644～651.

Thrun, S., Martin, C., Liu, Y., Hahnel, D.,

Montemerlo, R., Chakrabarti, D. and Burgard, W., 2004, "A Real-Time Expectation-Maximization Algorithm for Acquiring Multiplanar Maps of Indoor Environments with Mobile Robots," *IEEE Trans. on Robots and Automation*, Vol. 20, pp. 433～442.

Wijk, O. and Christensen, H. I., 2000, "Triangulation-Based Fusion of Sonar Data with Application in Robot Pose Tracking," *IEEE Trans. on Robotics and Automation*, Vol. 16, No. 6, pp. 740～752.